Electron Transport through a Self-Assembled Monolayer of Thiol-End-Functionalized Tetraphenylporphines and Metal Tetraphenylporphines

ARTICLE *in* LANGMUIR · APRIL 2006

Impact Factor: 4.46 · DOI: 10.1021/la052051l · Source: PubMed

10 AUTHORS, INCLUDING:

Hongxiang li
Chengdu University Of Traditional Chinese M...
104 PUBLICATIONS **2,585** CITATIONS
SEE PROFILE

Cai-Ming Liu
Chinese Academy of Sciences
154 PUBLICATIONS **3,054** CITATIONS
SEE PROFILE

Electron Transport through a Self-Assembled Monolayer of Thiol-End-Functionalized Tetraphenylporphines and Metal Tetraphenylporphines

Xiaoquan Lu,*,† Minrui Li,† Chunhe Yang,‡ Limin Zhang,† Yongfang Li,‡ Lang Jiang,‡ Hongxiang Li,‡ Lei Jiang,‡ Caiming Liu,‡ and Wenping Hu*,‡

College of Chemistry and Chemical Engineering, Northwest Normal University, Lanzhou 730070, PR China, and Laboratory of Organic Solids, Institute of Chemistry, Chinese Academy of Sciences, Beijing 100080, PR China

Received July 28, 2005. In Final Form: December 14, 2005

The monolayers of several thiol-end-functionalized tetraphenylphophines (SH−TPP) and metal tetraphenylporphines (SH−MTPP) were self-assembled on gold surfaces and identified by cyclic voltammetry (CV), electrochemical impedance spectroscopy, scanning electrochemical microscopy, and the contact angle. The CV peaks of the $[Fe(CN)_6]^{3-}$/$[Fe(CN)_6]^{4-}$ couple were used to identify the efficiency of electrons transferring through the self-assembled monolayer (SAM). The results suggested that SH−TPP and SH−MTPP could form high-quality SAMs on gold surfaces. The SAMs blocked electron transport from the gold electrode to solution. When the length of the thiol-end-link spacer (alkyl group) increased, the electron transport ability of the SAM decreased because of the increased insulator properties of the alkyl chain. With the insertion of metallic ions, the electron transport ability of the SAM of SH−MTPP increased compared to that of the SAM of SH−TPP, which was probably due to the fact that (i) the insertion of metallic ions changed the molecular structure and the molecular structure of SH−MTPP played an important role in electron transport through the SAM and (ii) the insertion of metallic ions increased the electron tunneling probability through the monolayer.

1. Introduction

Porphyrins have attracted particular attention recently because of their excellent stability and unique optical and electronic properties.[1] Moreover, the assembled ordered porphyrins exist widely in nature, such as in photosynthetic proteins serving as the active species in the initial steps of light-energy conversion.[2] Therefore, research on the self-assembled structures of porphyrins is not only attractive for clarifying the light-energy conversion mechanism of ordered porphyrins and further mimicking their functions but also represents a powerful method for the precise surface chemical modification of molecular and electronic devices, energy harvesting, storage, catalysis, and sensors.[3]

The self-assembled monolayer (SAM) is the first step in all assembly and interface engineering, hence it has attracted particular attention recently.[4] It is well known that thiols and disulfides can covalently link to gold surfaces by Au−S linkages to form highly ordered SAMs,[5] and several strategies have been used to prepare such SAMs.[6] However, to our knowledge few studies have addressed the electron transport ability through the SAM and the influence of the porphyrin center ions on electron transport (the center ions coordinated with the pyrrole units). Here we concentrate on these and study them by an electrochemical method. The results suggest that the thiol-end-functionalized tetraphenylphophines (SH−TPP) can form high-quality SAMs on gold surfaces, which block electron transport from the gold electrode to solution. When the length of the thiol-end-link spacer (alkyl group) increases, the electron transport ability of the SAMs decreases because of the increased insulator properties of the alkyl chain. With the insertion of metallic ions into the center of SH−TPP, the electron transport ability of the SAMs of metal tetraphenylporphines (SH−MTPP) increases.

2. Experiment

The synthesis of SH−TPP and SH−MTPP (Scheme 1) was described elsewhere.[7] Porphyrins were dissolved in chloroform (1 mM) and assembled on a precleaned gold disk electrode (with a diameter around 0.25 cm). The disk electrodes were polished carefully

* To whom correspondence should be addressed. E-mail: luxq@nwnu.edu.cn, huwp@iccas.ac.cn.

† Northwest Normal University.

‡ Chinese Academy of Sciences.

(1) (a) Falk, J. E. *Porphyrins and Metalloporphyrins*; Elsevier: Amsterdam, 1964. (b) Smith, K. M. *Porphyrins and Metalloporphyrins*; Elsevier: Amsterdam, 1975. (c) Dolphin, D. *The Porphyrins*; Academic Press: New York, 1978. (d) Nalwa, H. S. *Adv. Mater.* **1993**, *5*, 341−358. (e) Giraudeau, A.; Fan, F. F.; Bard, A. J. *J. Am. Chem. Soc.* **1980**, *102*, 5137−5142. (f) Kampas, F. J.; Yamashita, K.; Fajer, J. *Nature* **1980**, *284*, 40−42. (g) Chau, L.-K.; Arbour, C.; Collins, G. E.; Nebesny, K. W.; Lee, P. A.; England, C. D.; Armstong, N. R.; Barkinson, B. A. *J. Phys. Chem.* **1993**, *97*, 2690−2698. (h) Schlettwein, D.; Kaneko, M.; Yamada, A.; Wohrle, D.; Jaeger, N. I. *J. Phys. Chem.* **1991**, *95*, 1748−1755. (i) Cook, M. J. *Chem. Rec.* **2002**, *2*, 225−236.

(2) (a) Gust D.; Moore, T. A.; Moore, A. L. *Abstract of Papers of the American Chemical Society* **2004**, *228*, U53−U53 207-ORGN Part 2. (b) Kobuke, Y.; Ogawa, K. *Bull. Chem. Soc. Jpn.* **2003**, *76*, 689−708. (c) Huber, M. *Eur. J. Org.* Chem. **2001**, 4379−4389. (d) Dieks, H.; Senge, M. O.; Kirste, B.; Kurreck, H. *J. Org. Chem.* **1997**, *62*, 8666−8680. (e) Kurreck H.; Huber, M. *Angew. Chem., Int. Ed. Engl.* **1995**, *34*, 849−866. (f) Cao, Y.; Zhang, B. W.; Qian, W. Y.; Wang, X. D.; Bai, J. W.; Xiao, X. R.; Jia, J. G.; Xu, J. W. *Sol. Energy Mater. Sol. Cells* **1995**, *38*, 139−155.

(3) (a) Araki, K.; Angnes, L.; Azevedo, C. M. N.; Toma, H. E. *J. Electroanal. Chem.* **1995**, *397*, 205−210. (b) Araki, K.; Angnes, L.; Toma, H. E. *Adv. Mater.* **1995**, *7*, 554−559. (c) Malinski, T.; Taha, Z. *Nature* **1992**, *358*, 676−678. (d) Kolesar, E. S., Jr.; Wiseman, J. M. *Anal. Chem.* **1989**, *61*, 2355−2361. (e) Lefevre, D.; Porteu, F.; Balog, P.; Roulliay, M.; Zalczer, G.; Palacin, S. *Langmuir* **1993**, *9*, 150−161. (f) Mirsky, V. M. *TrAC, Trends Anal. Chem.* **2002**, *21*, 439−450. (g) Gooding, J. J.; Mearns, F.; Yang, W.; Liu, J. *Electroanalysis* **2003**, *15*, 81−96. (h) Schoen, J. H.; Meng, H.; Bao, Z. *Adv. Mater.* **2002**, *14*, 323−326. (i) Roth, K. M.; Gryko, D. T.; Clausen, C.; Li, J.; Lindsey, J. S.; Kuhr, W. G.; Bocian, D. F. *J. Phys. Chem. B* **2002**, *106*, 8639−8648. (j) Tsuda, A.; Sakamoto, S.; Yamaguchi, K.; Aida, T. *J. Am. Chem.* Soc. **2003**, *125*, 15722−15723. (k) Taylor, P. N.; Anderson, H. L. *J. Am. Chem. Soc.* **1999**, *121*, 11538−11545. (l) Li, Q.; Mathur, G.; Gowda, S.; Surthi, S.; Zhao, Q.; Yu, L.; Lindsey, J. S.; Bocian, D. F.; Misra, V. *Adv. Mater.* **2004**, *16*, 133−137. (m) Yamada, H.; Imahori, H.; Nishimura, Y.; Yamazaki, I.; Ahn, T. K.; Kim, S. K.; Kim, D.; Fukuzumi, S. *J. Am. Chem. Soc.* **2003**, *125*, 9129−9139. (n) He, Y. F.; Ye, T. Borguet, E. *J. Am. Chem. Soc.* **2002**, *124*, 11964−11970. (o) Wang, Z. C.; Medforth, C. J.; Shelnutt, J. A. *J. Am. Chem. Soc.* **2004**, *126*, 15954−15955.

10.1021/la052051l CCC: $33.50
Published on Web 03/01/2006

Scheme 1. Molecular Structure of SH−TPP and SH−MTPP (M=Fe, Zn and Ni)

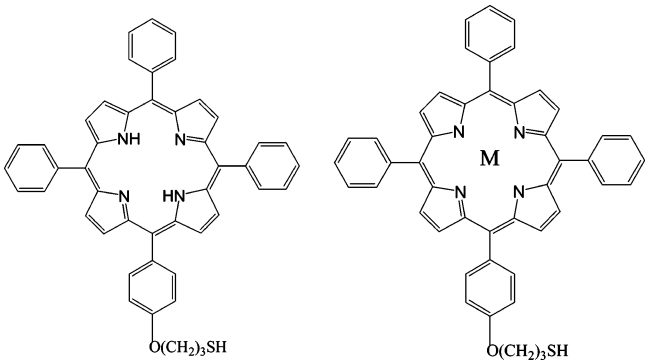

and cleaned with pure water four times and finally treated with oxygen plasma for 15 s. SAMs were identified by cyclic voltammetry (CV), electrochemical impedance spectroscopy (EIS) (Zahner IM6e electrochemical work station (Germany)), scanning electrochemical microscopy (SECM, CHI 900, USA), and the contact angle (Data Physical SCA20, Germany).

3. Results and Discussion

The self-assembly of SH−TPP on a gold electrode was monitored by CV. $[Fe(CN)_6]^{3-}/[Fe(CN)_6]^{4-}$ couple peaks were used to identify the electron-transfer efficiency through the SAMs. With SH−TPP molecules bounded to the gold surface step by step, electron transport was blocked gradually.[8] It appeared on CVs as $[Fe(CN)_6]^{3-}/[Fe(CN)_6]^{4-}$ peak currents decreasing and becoming more and more irreversible (as shown in Figure 1A). The Nyquist plots of the ac impedance displayed with SH−TPP adsorption the increasing resistance of the SAM (EIS, Figure 1B). After 30 min, the peak current of the CV was suppressed to its lowest value, and then small changes in current and resistance were observed even though the assembly time was prolonged, which indicated that the SAM reached saturation. The saturation

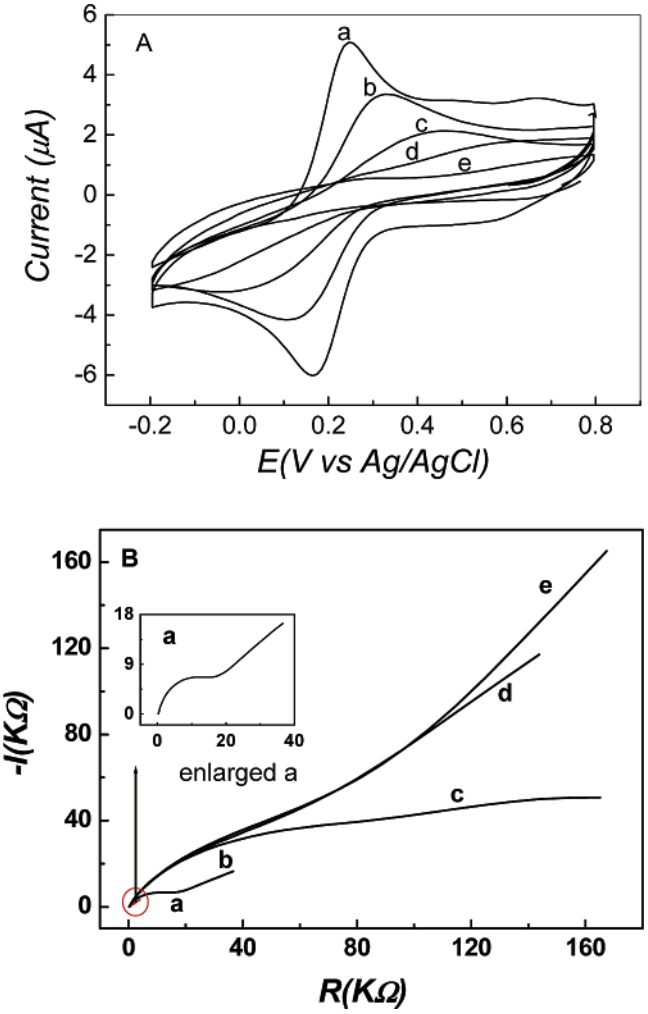

Figure 1. CVs (A) and ac impedance plots (B) of a gold electrode modified with SH−TPP at different times—(a) bare Au, (b) 5 min, (c) 10 min, (d) 20 min, (e) 30 min—in a 5 mM $[Fe(CN)_6]^{3-}$/0.05 M KCl aqueous solution. The scan rate is 50 $mV \cdot s^{-1}$.

of the SAM was further demonstrated by SECM results. The SECM images suggested that the SAM of SH−TPP was formed after 30 min (Figure 2). Area B of the gold electrode covered by SH−TPP was calculated to be around 99%[8a] in this case ($B = 1 - [i_p^f(SH-TPP)/i_p^f(Au)]$, where, $i_p^f(SH-TPP)$ and $i_p^f(Au)$ are the reduction peak currents of ferricyanide on the Au−SH−TPP and Au electrodes, respectively).

It is obvious from Scheme 1 that SH−TPP is an amphiphilic molecule. After the hydrophilic −SH end attaches to the Au electrode, the hydrophobic phenyl ring will stretch out on the surface (Figure 3a). If the SAM of SH−TPP reaches saturation, then the wettability of the surfaces before and after assembly should be changed.[9] The results of the contact angle of Au and Au−SAM surfaces definitely confirmed this (Figure 3b and c); the contact angle changed more than 30° before and after self-assembly. It is interesting that a SAM could change the surface wettability so greatly, which suggests potential applications of SAMs in surface engineering.

Considering the wide existence and application of metal porphyrins in surface engineering and photo/electrical devices, it will be very interesting to know the self-assembly states of metal tetraphenylporphines (SH−MTPP) so that we can compare them with those of SH−TPP to reveal the role that metallic ions

(4) (a) Luttrull, D. K.; Graham, J.; DeRose, J. A.; Gust, D.; Moore, T. A.; Lindsay, S. M. *Langmuir* **1992**, *8*, 765−768. (b) Han, W.; Li, S.; Lindsay, S. M.; Gust, D.; Moore, T. A.; Moore, A. L. *Langmuir* **1996**, *12*, 5742−5744. (c) Simpson, T. R. E.; Revell, D. J.; Cook, M. J.; Russell, D. A. *Langmuir* **1997**, *13*, 460−464. (d) Katz, E.; Willner, I. *Langmuir* **1997**, *13*, 3364−3373. (e) Yuan, H.; Woo, L. K. *J. Porphyrins Phthalocyanines* **1997**, *1*, 189−200. (f) Imahori, H.; Azuma, T.; Ushida, K.; Takahashi, M.; Akiyama, T.; Hasegawa, M.; Okada, T.; Sakata, Y. *SPIE* **1997**, *3142*, 104−111. (g) Uosaki, K.; Kondo, T.; Zhang, X.-Q.; Yanagida, M. *J. Am. Chem. Soc.* **1997**, *119*, 8367−8368. (h) Crossley, M. J.; Prashar, J. K. *Tetrahedron Lett.* **1997**, *38*, 6751−6754. (i) Imahori, H.; Norieda, H.; Ozawa, S.; Ushida, K.; Yamada, H.; Azuma, T.; Tamaki, K.; Sakata, Y. *Langmuir* **1998**, *14*, 5335−5338. (j) McDermott, M. T.; Green, J. B. D.; Porter, M. D. *Langmuir* **1997**, *13*, 2504−2510. (k) Imahori, H.; Hosomizu, K.; Mori, Y.; Sato, T.; Ahn, T.; Kim, S. K.; Kim, D.; Nishimura, Y.; Yamazaki, I.; Ishii, H.; Hotta, H.; Motano, Y. *J. Phys. Chem. B* **2004**, *108*, 5018−5025. (l) Ashkenasy, G.; Kalyuzhny, G.; Libman, J.; Rubinstein, I.; Shanzer, A. *Angew. Chem., Int. Ed.* **1999**, *38*, 1257−1261. (m) Zhang, Z. J.; Hou, S. F.; Zhu, Z. H.; Liu, Z. F. *Langmuir* **2000**, *16*, 537−540. (n) Boeckl, M. S.; Bramblett, A. L.; Hauch, K. D.; Sasaki, T.; Ratner, B. D.; Rogers, J. W., Jr. *Langmuir* **2000**, *16*, 5644−5653. (o) Ni, Y. H.; Puthenkovilakom, R. R.; Hou, Q. *Langmuir* **2004**, *20*, 2765−2771.

(5) (a) Ulman, A. *Chem. Rev.* **1996**, *96*, 1533−1554. (b) Tour, J. M. *Chem. Rev.* **1996**, *96*, 537−554. (c) Tour, J. M.; Jones, L., II; Pearson, D. L.; Lamba, J. J. S.; Burgin, T. P.; Whitesides, G. M.; Allara, D. L.; Parikh, A. N.; Atre, S. V. *J. Am. Chem. Soc.* **1995**, *117*, 9529−9534. (d) Whitesides, G. M.; Mathias, J. P.; Seto, C. T. *Science* **1991**, *254*, 1312−1319. (e) Zareie, M. H.; Ma, H.; Reed, B. W.; Jen, A. K. Y.; Sarikaya, M. *Nano Lett.* **2003**, *3*, 139−142.

(6) (a) Zak, J.; Yuan, H. P.; Ho, M.; Woo, L. K.; Porter, M. D. *Langmuir* **1993**, *9*, 2772−2774. (b) Hutchison, J. E.; Postlehwaite, T. A.; Murray, R. W. *Langmuir* **1993**, *9*, 3277−3283. (c) Postlehwaite, T. A.; Hutchison, J. E.; Hathcock, K. W.; Murray, R. W. *Langmuir* **1995**, *11*, 4109−4116. (d) Hutchison, J. E.; Postlehwaite, T. A.; Chen, C.-H.; Hathcock, K. W.; Ingram, R. S.; Ou, W.; Linton, R. W.; Murray, R. W. *Langmuir* **1997**, *13*, 2143−2148. (e) Guo, L.-H.; Mclendon, G.; Razafitrimo, H.; Gao, Y. L. *J. Mater. Chem.* **1996**, *6*, 369−374.

(7) (a) Cordas, C. M.; Viana, A. S.; Lcupold, S.; Montforts, F.-P.; Abrantes, L. M. *Electrochem. Commun.* **2003**, *5*, 36−41. (b) Lu, X.; Lu, B.; Xue, Z.; Zhang, M.; Wang, Y.; Kang, J. *Anal. Lett.* **2002**, *35*, 1811−1822.

(8) (a) Bollo, S.; Yáñez, C.; Sturm, J.; Núñez-Vergara, L.; Squella, J. *Langmuir* **2003**, *19*, 3365−3370. (b) Nahir, T. M. *Langmuir* **2002**, *18*, 5283−5286.

(9) Roucoules, V.; Gaillard, F.; Mathia, T. G.; Lanteri, P. *Adv. Colloid Interface Sci.* **2002**, *97*, 179−203.

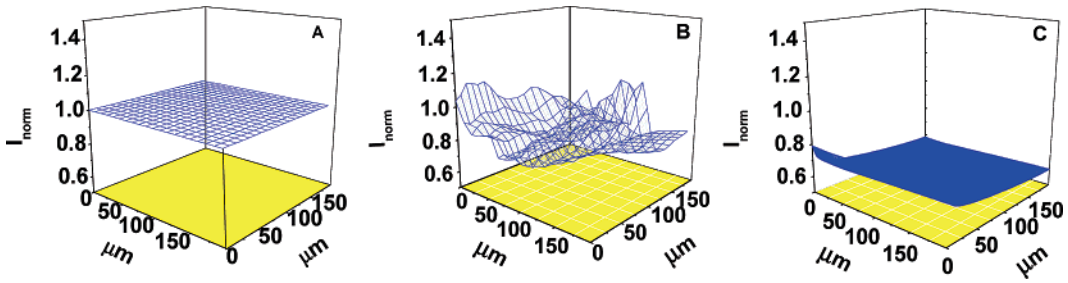

Figure 2. SECM images of (A) bare gold and self-assembled SH−TPP at after (B) 15 min and (C) 30 min.

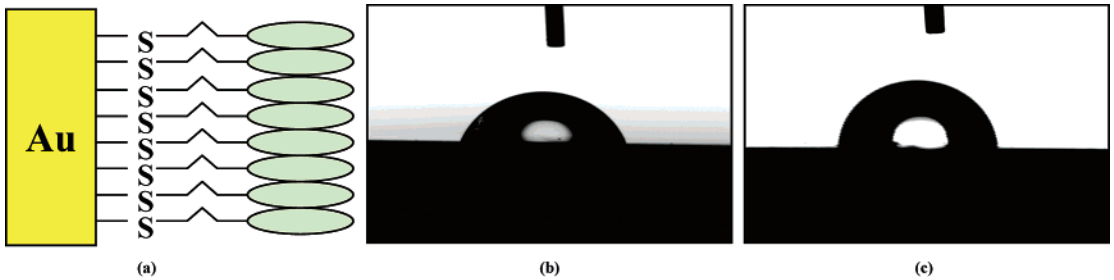

Figure 3. (a) SAM model of SH−TPP. (b) Contact angle of the bare gold surface is ∼50°. (c) Contact angle of the Au−SAM surface is ∼84°.

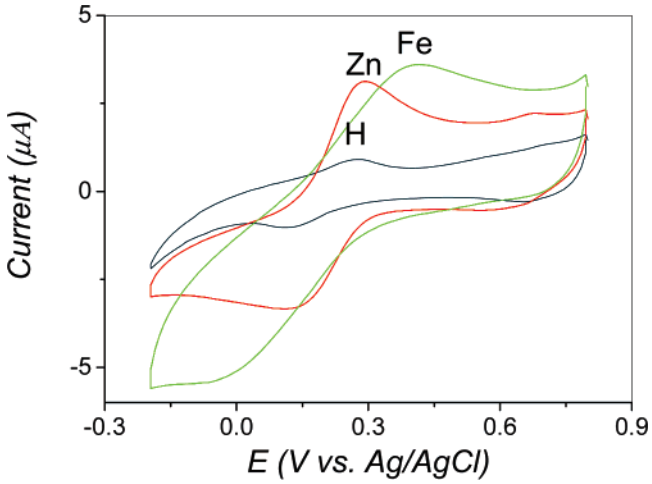

Figure 4. CVs of SH−FeTPP and SH−ZnTPP SAM in a 0.05 M KCl aqueous solution containing 5 mM $[Fe(CN)_6]^{3-}$, where the scan rate is 50 mV·s^{-1}. Here the plots of SH−TPP were used for reference.

play in electron transfer. With this aim, SAMs of SH−MTPP (M = Fe^{2+}, Zn^{2+}) were assembled and characterized by SECM and contact angles, and results similar to those for SH−TPP were demonstrated. However, the CVs of SH−MTPP (M = Fe^{2+}, Zn^{2+}) were much different from those of SH−TPP (Figure 4); peak currents follow the order SH−FeTPP > SH−ZnTPP > SH−TPP.

As we know, the peak currents in CV result from the reduction of $[Fe(CN)_6]^{3-}$ on the gold surface (the potential was low enough in the case of the reaction of porphyrins, Fe^{2+}, Zn^{2+}); therefore, the peak current was proportional to the electron availability of $[Fe(CN)_6]^{3-}$ from the electrode. Electrons can be made available in two ways: The first is from the gold electrode directly through the space between two porphyrin molecules or from the defect of the monolayer. The second is from the SAM surface where electrons tunnel through the SAM. As we know, the FeTPP macro-ring has a distorted structure (Figure 5, top picture),[10] which easily results in a large distance between the neighboring molecules of FeTPP (Figure 5a, bottom picture) so that the distance between two neighbored molecules is around 8.317 Å (the center Fe−Fe distance). However, ZnTPP and TPP have planar structures (Figure 5b and c), and the planar distances are 6.443 and 6.440 Å,[11] respectively. It is reasonable to deduce that the distorted structure and large distance between FeTPP molecules increase the electron availability of $[Fe(CN)_6]^{3-}$ through the molecular space of the monolayer. To confirm this, we synthesized other MTPP, thiol-end-functionalized nickel tetraphenylporphines (SH−NiTPP, alkyl length $n_{carbon} = 3$) for the experiments. We selected SH−NiTPP as the candidate because the NiTPP molecule has a similar distortion structure and a neighboring molecular distance (Ni−Ni, 8.290 Å) that is similar to that of FeTPP.[12] As expected, the SH−NiTPP monolayer exhibited results similar to those for SH−FeTPP,as and the peak current of SH−NiTPP > SH−ZnTPP > SH−TPP, which indicates that the molecular structure of SH−MTPP plays an important role in electron transport through the SAM.

However, although ZnTPP and TPP have similar planar structures (Figure 5b and c) and similar planar distances (ZnTPP: 6.443 Å; TPP: 6.440 Å), the CVs of SH−ZnTPP and SH−TPP are still different (Figure 4). The reason is possibly due to the different electron transport ability of the SH−ZnTPP and SH−TPP molecules. As we mentioned above, the peak current of CVs is proportional to the electron availability of $[Fe(CN)_6]^{3-}$ from the electrode. The electrons are available in two ways: The first is from the gold electrode directly through inter-porphyrin molecular space or from the defect of the monolayer. The second is from the SAM surface where electrons are transported through the monolayer. It is well known that the geometry of the orbitals on the sulfurs does not permit the π orbitals from porphyrin molecules to interact strongly with the conduction orbitals of the

(10) (a) Collman, J. P.; Hoard, J. L.; Kim, N.; Lang, G.; Reed, C. A. *J. Am. Chem. Soc.* **1975**, *97*, 2676−2681. (b) Li, N.; Su, Z.; Coppens, P.; Landrum, J. *J. Am. Chem. Soc.* **1990**, *112*, 7294−7298.

(11) (a) Byrn, M. P.; Curtis, C. J.; Hsiou, Y.; Khan, S. I.; Sawin, P. A.; Tendick, S. K.; Terzis, A.; Strouse, C. E. *J. Am. Chem.* Soc. **1993**, *115*, 9480−9497. (b) Scheidt, W. R.; Mondal, J. U.; Eigenbrot, C. W.; Adler, A.; Radonovich, L. J.; Hoard, J. L. *Inorg. Chem.* **1986**, *25*, 795−799. (c) Hamor, M. J.; Hamor, T. A.; Hoard, J. L. *J. Am. Chem. Soc.* **1964**, *86*, 1938−1942. (d) Silvers, S. J.; Tulinsky, A. *J. Am. Chem. Soc.* **1967**, *89*, 3331−3337. (e) Kano, K.; Fukuda, K.; Wakami, H.; Nishiyabu, R.; Pasternack, R. *J. Am. Chem. Soc.* **2000**, *122*, 7494−7502.

(12) Fleischer, E. B.; Miller, C. K.; Webb, L. E. *J. Am. Chem. Soc.* **1964**, *86*, 2342−2347.

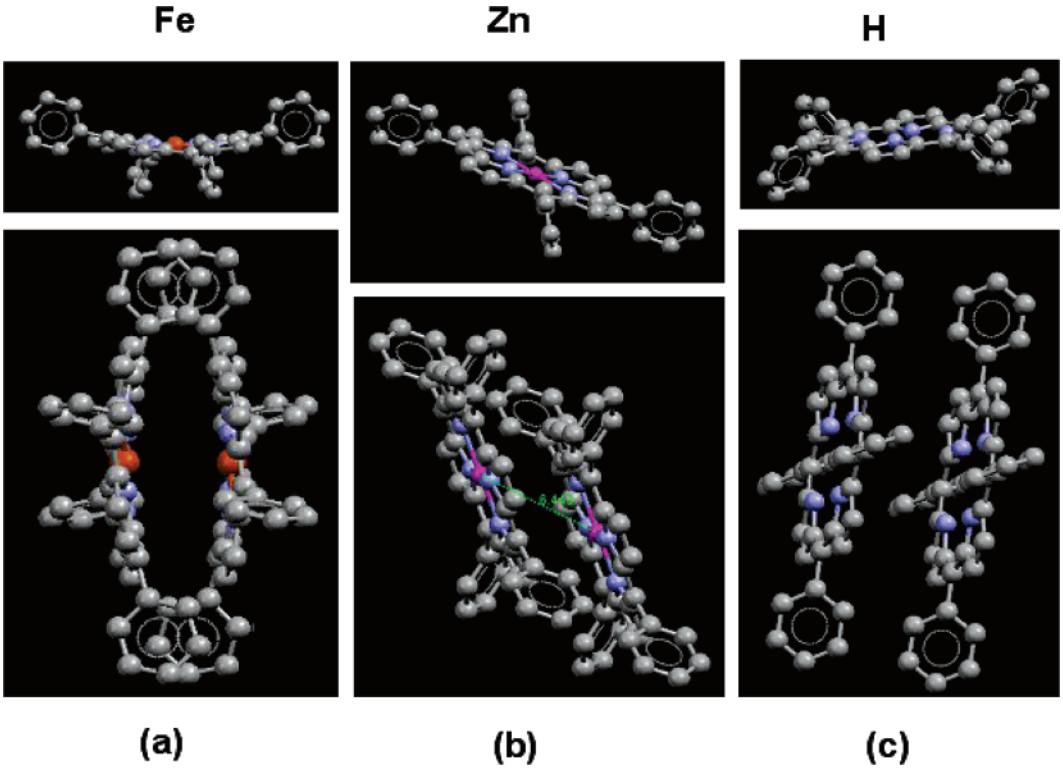

Figure 5. Structures of (a) SH−FeTPP, (b) SH−ZnTPP, and (c) SH−TPP and the stacking between neighboring molecules.

gold surfaces, so the orbital mismatch creates a potential barrier at the interface of the Au/SAM. It is well known that carrier injection through a bond is usually induced by a tunneling mechanism.[13] A number of recent reports have appeared on electron tunneling phenomena in the thiol-based Au/SAM interface.[13] Therefore, in our SAMs it is highly possible that electrons are transported through them by tunneling. To confirm this, nanojunctions of Au/prophyrins/Au were fabricated according to a previous description.[14] The current−voltage characteristics (*IV*s) of the nanojunctions exhibited nonlinear characteristics and a very weak temperature dependence between 267 and 297 K. The nonlinear *IV*s suggested the possible tunneling mechanism of electron transport through the SAM,[13,14] and the weak temperature dependence indicated that there is no obvious thermal activation process in the carrier injection. Moreover, the observed *IV*s did not fit the thermal emission and space-charge-limited current models, indicating that the electrons are caused by the tunneling mechanism. Furthermore, the existence of the tunneling mechanism for electron transport through the SAM was proven by adjusting the length of SAM link spacers to observe

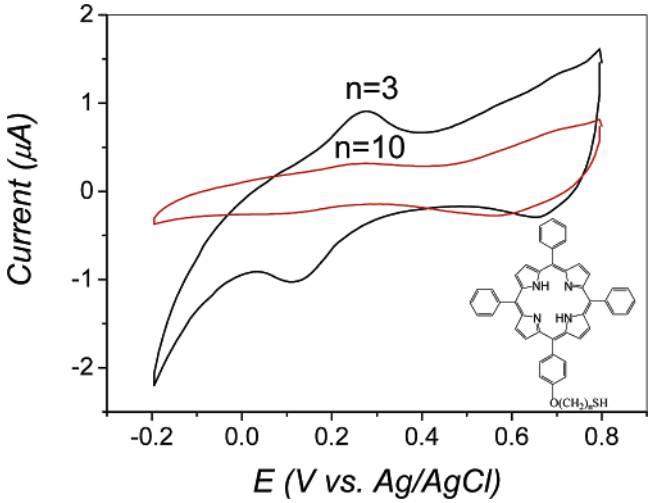

Figure 6. CVs of the SH−TPP SAM with different link spacers ($n = 3$, $n = 10$) in a 0.05 M KCl aqueous solution containing 5 mM $[Fe(CN)_6]^{3-}$, where the scan rate is 50 mV·s^{-1}.

the change in the peak currents of CVs. With the length of the link spacer increasing ($n = 3 \rightarrow 10$, to change the length of the tunneling barrier), the peak currents of the CVs decreased sharply (Figure 6), which should be due to the increased insulating properties of the long alkyl chain resulting in a low electron tunneling probability through the SAM.[15] Therefore, the tunneling mechanism of electrons transport through the SAMs definitely exists. Now, let us temporarily assume that the SAM is compact and and has no defects so that electrons can be transported through the SAM only by tunneling. In this case, electrons are transported

(13) (a) Reed, M. A.; Zhou, C.; Muller, C. J.; Burgin, T. P.; Tour, J. M. *Science* **1997**, *278*, 252−254. (b) Chen, J.; Reed, M. A.; Rawlett, A. M.; Tour, J. M. *Science* **1999**, *286*, 1550−1552. (c) Hong, S.; Reifenberger, R.; Tian, W.; Datta, S.; Henderson, J.; Kubiak, C. P. *Superlattices Microstruct.* **2000**, *28*, 289−303. (d) Andres, R. P.; Bein, T.; Dorogi, M.; Feng, S.; Henderson, J. I.; Kubiak, C. P.; Mahoney, W.; Osifchin, R. G.; Reifenberger, R. *Science* **1996**, *272*, 1323−1325. (e) Kushemerick, J. G.; Holt, D. B.; Yang, J. C.; Naciri, J.; Moore, M. H.; Shashidhar, R. *Phys. Rev. Lett.* **2002,** *89*, 086802. (f) Kergueris, C.; Bourgoin, J. P.; Palacin, S.; Esteve, D.; Urbina, C.; Magoga, M.; Joachim, C. *Phys. Rev. B* **1999**, *59*, 12505−12513. (g) Yaliraki, S. N.; Kemp, M.; Ratner, M. A. *J. Am. Chem. Soc.* **1999**, *121*, 3428−34. (h) Nitzan, A. *Annu. Rev. Phys. Chem.* **2001**, *52*, 681−750. (i) Hettler, M. H.; Schoeller, H.; Wenzel, W. *Europhys. Lett.* **2002**, *57*, 571−577. (j) Petrov, E. G.; Haenggi, P. *Phys. Rev. Lett.* **2001**, *86*, 2862. (k) Weber, H. B.; Reichert, J.; Weigend, F.; Ochs, R.; Beckmann, D.; Mayor, M.; Ahlrichs, R.; Loehneysen, H. *Chem. Phys.* **2002**, *281*, 113−125. (l) Mujica, V.; Nitzan, A.; Datta, S.; Ratner, M. A.; Kubiak, C. P. *J. Phys. Chem. B* **2003**, *107*, 91−95. (m) Xu, B. Q.; Tao, N. J. *Science* **2003**, *301*, 1221−1223. (n) Cui, X. D.; Primak, A.; Zarate, X.; Tomfohr, J.; Sankey, O. F.; Moore, A. L.; Moore, T. A.; Gust, D.; Harris, G.; Lindsay, S. M. *Science* **2001**, *294*, 571−574. (o) Wang, W.; Lee, T.; Reed, M. A. *Phys. Rev. B* **2003**, *68*, 035416.

(14) Hu, W. P.; Nakashima, H.; Furukawa, K.; Kashimura, Y.; Ajito, K.; Han, C. X.; Torimitsu, K. *Phys. Rev. B* **2004**, *69*, 165207.

(15) (a) Kobayashi, S.; Nishikawa, T.; Takanobu, T.; Mori, S.; Shimoda, T.; Mitani, T.; Shimotani, H.; Yoshimoto, N.; Ogawa, S.; Iwasa, Y. *Nat. Mater.* **2004**, *3*, 317−322. (b) Collet, J.; Tharaud, O.; Chapoton, A.; Vuillaume, D. *Appl. Phys. Lett.* **2000**, *76*, 1941−1943. (c) Halik, M.; Klauk, H.; Zschieschang, U.; Schmid, G.; Dehm, C.; Schutz, M.; Maisch, S.; Effenberger, F.; Brunnbauer, M.; Stellacci, F. *Nature* **2004**, *431*, 963−966.

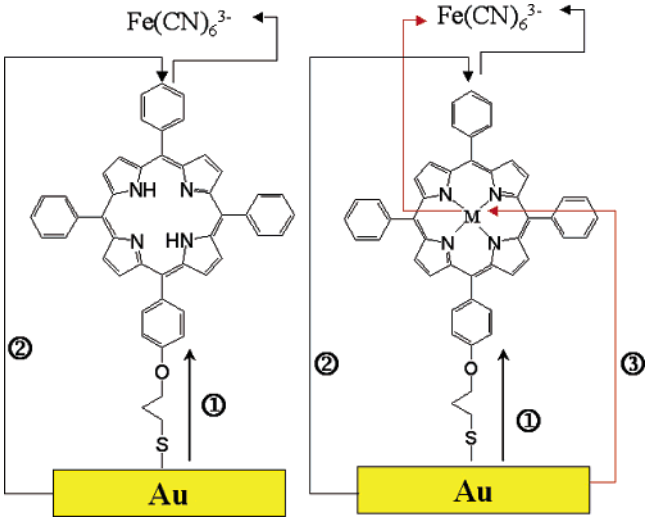

Figure 7. Assumed electron-transfer processes of perfect SAMs of SH−TPP and SH−MTPP: (1) From the gold electrode through the alkyl chain to the porphyrin macro-ring and then transfer to $[Fe(CN)_6]^{3-}$; (2) from the gold electrode to the surface of the SAM directly and then transfer to $[Fe(CN)_6]^{3-}$, and (3) from the gold electrode to the center M and then transfer to $[Fe(CN)_6]^{3-}$.

through the SAM in two ways: (1) from the Au electrode tunnel through the alkyl bridge and then through the macro-ring and finally to $[Fe(CN)_6]^{3-}$ and (2) from the Au electrode through the SH−TPP monolayer directly to $[Fe(CN)_6]^{3-}$ (Figure 7, left). With the insertion of metallic ions into porphyrin center electrons, transport through the SAM of SH−MTPP probably has a new possibility: (3) (Figure 7, right) from the Au electrode to the metallic ion and then via transfer to $[Fe(CN)_6]^{3-}$. Recently, Park et al. found one Co ion bonded to two terpyridinyl linker molecules with thiol end groups, and electron transport was through the center Co.[16] Our molecules of SH−ZnTPP were similar to Park's structure, and similar electron transport probably takes place in the SH−ZnTPP monolayer (i.e., through the center metallic ions as shown in Figure 7, right). By the way, with the insertion of metallic ions, the conductivity of the porphyrin macro ring increased, which probably also benefited the electron transport through the SAM.[17] Regardless of the detailed tunnel mechanism of electron transport through the SAMs, it is clear that the incorporated metallic ions increased the electron transport efficiency from the Au electrode to $[Fe(CN)_6]^{3-}$.

4. Summary

SH−TPP and SH−MTPP can form high-quality SAMs on gold surfaces. The $[Fe(CN)_6]^{3-}/[Fe(CN)_6]^{4-}$ couple peaks were used to identify the electron-transfer efficiency through the SAMs. The SAM of SH−TPP blocked the electron transport from the gold electrode to solution. However, with the insertion of metallic ions into the center of SH−TPP, the reduction currents of $[Fe(CN)_6]^{3-}$ on the gold electrode were increased because of the increased electron transport probability. The increased electron transport probability can be understood in two different ways: (1) the insertion of metallic ions resulting in the distortion of porphyrin molecules, where the molecular structure of SH−MTPP played an important role in electron transport through the SAM and (2) the insertion of metallic ions increased the electron tunneling probability.

Acknowledgment. We acknowledge financial support from the Natural Science Foundation of China (20335030, 20404013, and 20527001), Ministry of Education of China, Ministry of Chinese Science and Technology and Chinese Academy of Sciences.

LA052051L

(16) Park, J.; Pasupathy, A. N.; Goldsmith, J. I.; Chang, C.; Yaish, Y.; Petta, J. R.; Rinkoski, M.; Sethna, J. P.; Abruna, H. D.; McEuen, P. L.; Ralph, D. C. *Nature* **2002**, *417*, 722−725.

(17) (a) Zhang, X. Q.; Cheng, Z. P.; Wu, H. M.; Wu, X. J. *Synth. Met.* **1996**, *82*, 71−74. (b) Zhang, X. Q.; Wu, H. M.; Wei, Y.; Cheng, Z. P.; Wu, X. J. *Solid State Commun.* **1995**, *95*, 99−101.